The dispersion of ^{137}Cs and $^{239,240}Pu$ in the Rhone River plume: a numerical model

R. Periáñez *

Dpto. Física Aplicada I, E.U. Ingeniería Técnica Agrícola, Universidad de Sevilla, Ctra. Utrera km 1, 41013 Sevilla, Spain

Abstract

A numerical three dimensional model to simulate the transport of Cs and Pu by the Rhone River plume has been developed. The model solves the hydrodynamic equations, including baroclinic terms (that account for density variations) and a turbulence model, the suspended matter equations, including several particle classes simultaneously, settling, deposition and erosion of the sediment, and the radionuclide dispersion equations. Exchanges of radionuclides between the liquid and solid phases are described in terms of kinetic transfer coefficients. The dependence of these coefficients with water salinity is explicitly included in the model since it changes from freshwater to seawater values in the model domain. Computed activity levels in water, suspended matter and bed sediments are, in general, in agreement with measurements in the area. The model can also give a wide amount of information, as distribution coefficients for total suspended matter and sediments and for each particle class, fractions of radionuclides fixed to solid particles, and vertical profiles of radionuclides and distribution coefficients.

Keywords: Rhone River; Caesium; Plutonium; Numerical modelling; Sediment; Suspended matter; Dispersion

1. Introduction

There has been an increasing interest in the development of marine dispersion models for radionuclides since they can be applied in the assessment of the radiological consequences of existing or planned routine discharges, as well as in the

* Tel.: +34-954-486474; fax: +34-954-486436.
E-mail address: rperianez@us.es (R. Periáñez).

case of accidental releases. Also, useful oceanographic information can be obtained from the application of radionuclide dispersion models. Thus, very good models that can simulate the dispersion of nonconservative radionuclides in the marine environment have been recently described (see for instance Aldridge et al., 2003; Margvelashvily et al., 1997; Goshawk et al., 2003; Nakano and Povinec, 2003). These models represent an improvement in the description of radionuclide dispersion with respect to the earlier box models in which advective/diffusive transport was parameterized in terms of effective transfer coefficients (see for instance Nielsen, 1995).

In this paper, a model for simulating the transport of radionuclides in a river plume is described and applied to the Rhone River plume, which introduces radionuclides released to the river into the Mediterranean Sea. The model domain covers all the river plume in the coastal area, where salinity changes from freshwater to seawater values. Artificial radionuclides reach the Rhone River through weathering of surface soils contaminated by atmospheric fallout and through the effluents from nuclear facilities: several power plants located along the river course and, mainly, from Marcoule nuclear fuel reprocessing plant (now is not in operation but releases have continued since washing effluents are produced and discharged). In the case of the Rhone, the low mixing of the discharge waters gives place to a well-identified surface plume in which a thin upper layer (1 or 2 m) is separated from the ambient seawater by a sharp density gradient. This plume extends 20 or 30 km offshore. Numerical modelling of these plumes is a difficult task that requires the inclusion of density differences in the full 3D hydrodynamic equations. The Rhone River gives the opportunity to test the behaviour of radionuclide dispersion models, including a kinetic approach for the transfers between the liquid and solid phases, when integrated with a detailed hydrodynamic model of a complex oceanographic system as a surface river plume.

It must be pointed out that some detailed models have already been developed to study the water circulation in the Rhone plume (Estournel et al., 1997; Marsaleix et al., 1998; Estournel et al., 2001). Also, some models describe the transport of sediments in the plume (Kondrachoff et al., 1994; Estournel et al., 1997), although in a rather simple way. Indeed, only one particle size was considered in these references and deposition was not included. However, a radionuclide dispersion model for any river plume, integrated with a hydrodynamic model and a detailed suspended sediment model, has not been described and tested before.

The model solves the hydrodynamic equations, including baroclinic terms that account for density variations and a turbulence model, and the suspended matter equations together with the radionuclide dispersion equations. The suspended matter equations include advective/diffusive transport of particles, settling (vertical fall), particle deposition on the seabed and erosion of the sediment. Several suspended matter particle classes are considered since a sensitivity study (Periáñez, 2004a) has indicated that model output is very sensitive to the particle size used in the equations. Exchanges of radionuclides between the liquid and solid phases are described in terms of kinetic coefficients. The dependence of kinetic coefficients with water salinity is also included in the model. This is necessary in a river plume

where salinity changes from freshwater to seawater values. The model has been applied to simulate the dispersion of ^{137}Cs and $^{239,240}Pu$ and results have been compared with measurements in the plume.

The model is described in the following section. Next, results are presented and discussed.

2. Material and methods: model description

2.1. Hydrodynamics and suspended particulate matter

Water circulation is obtained from the full three dimensional hydrodynamic equations, including baroclinic terms that account for density gradients (see for instance Kowalick and Murty, 1993). Water density is related with salinity through a standard equation of state (Kowalick and Murty, 1993) and salinity is computed from an advection/diffusion equation with appropriate boundary conditions at the river mouth. A 1-equation turbulence model is applied to determine the vertical eddy viscosity over the model domain (Davies and Hall, 2000). This type of turbulence model has also been used in Xing and Davies (1999) to simulate a river plume. Equations are quite standard and will not be repeated here.

Several suspended particle classes are considered in the model. Each particle class is governed by an advection/diffusion equation to which the settling, deposition and erosion terms are added. The settling velocity of each particle class is determined from Stokes's law applied to the average particle diameter of each class, as in other suspended sediment models (Cancino and Neves, 1999; Clarke and Elliott, 1998; Nicholson and O'Connor, 1986; Lumborg and Windelin, 2003). The deposition rate is written in terms of the settling velocity of particles and their concentration just above the sea bed (see for instance Nicholson and O'Connor, 1986; Holt and James, 1999; Liu et al., 2002a; Lumborg and Windelin, 2003; Wu et al., 1998; Prandle et al., 2000; Cancino and Neves, 1999). The erosion term for each particle class is written using the erodability constant and the fraction of particles of the corresponding class in the bed (Liu et al., 2002a, b; Cancino and Neves, 1999; Prandle et al., 2000; Holt and James, 1999; Nicholson and O'Connor, 1986). Critical erosion and deposition stresses are also used in the conventional form (see references above). Sedimentation rates are calculated as the balance between the deposition and erosion terms.

2.2. Radionuclide dispersion

It is considered that the exchanges of radionuclides between the liquid and solid phases are governed by a single reversible reaction. Thus, the transfer from the liquid to the solid phase is governed by a kinetic coefficient k_1 and the inverse process by a kinetic coefficient k_2 (dimensions $[T]^{-1}$). It is known that adsorption depends on the surface of particles per water volume unit at each point and time step. This quantity has been denoted as the exchange surface (Periáñez et al., 1996b; Periáñez and Martínez-Aguirre, 1997; Periáñez, 1999, 2000, 2002). Thus, the

kinetic coefficient $k_{1,i}$ is written as:

$$k_{1,i} = \chi_1 \left(S_{\mathrm{m},i} + S_{\mathrm{s},i} \right) = k_{11,i} + k_{12,i} \tag{1}$$

where S_{m} and S_{s} are the exchange surfaces for suspended matter and bottom sediments, respectively (dimensions $[L]^{-1}$) and χ_1 is a parameter with the dimensions of a velocity denoted as the exchange velocity (Periáñez et al., 1996b; Periáñez and Martínez-Aguirre, 1997; Periáñez, 1999, 2000, 2002). The index $i = 1 \ldots N$ is used to represent each one of the particle classes included in the model. Assuming spherical particles, the exchange surfaces are written as (see references cited above):

$$S_{\mathrm{m},i} = \frac{3 m_i}{\rho R_i} \tag{2}$$

and

$$S_{\mathrm{s},i} = \frac{3 L f_i \phi}{R_i \Upsilon} \tag{3}$$

where R_i and ρ are particle radius and density, respectively, m_i is suspended matter concentration, L is the sediment mixing depth (the distance to which the dissolved phase penetrates the sediment), Υ is the thickness of the water layer above the bed sediments that interacts with them, f_i is the fraction of particles of class i in the sediment and ϕ is a correction factor that takes into account that part of the sediment particle surface may be hidden by other sediment particles (thus, it is also related to sediment porosity). For simplicity, it has been assumed that Υ is equal to the vertical grid size: $\Upsilon = \Delta z$. This formulation has been successfully used in all modelling works cited above. Real particles are not spheres, but with this approach it is possible to obtain an analytical expression for the exchange surface (Duursma and Carroll, 1996).

The solid-solution partitioning of radionuclides is very sensitive to changes in salinity, with distribution coefficients decreasing with increasing salinity (Turner and Millward, 1994). The general theory of Abril and Fraga (1996) also predicts and inverse relationship between the distribution coefficients and salinity. The formulation given in Laissaoui et al. (1998) for the dependence of the exchange velocity upon salinity, which is deduced from the theory of Abril and Fraga (1996) is used:

$$\chi_1 = \chi_1^0 (1 - \delta) \tag{4}$$

where

$$\delta = \frac{S}{S + S_0} \tag{5}$$

In these equations, χ_1^0 is the freshwater value of the exchange velocity and S_0 is the salinity value at which 50% of saturation occurs (Laissaoui et al., 1998). It must be noted that as salinity increases, the transfer of radionuclides to the solid phase decreases due to competition effects of radionuclides with ions dissolved in

water. The relations given above have been tested through laboratory experiments (Laissaoui et al., 1998).

The kinetic coefficient k_2 is considered to be constant and to have the same value for all particle classes.

Recent work has shown that a kinetic model involving two consecutive reversible reactions (2-step model) may be more appropriate than that consisting of a single (1-step) reversible reaction, especially for long (months) water–sediment contact times (Periáñez, 2004b). However, given the time scale of simulations that are carried out (several days), it is not expected that significant differences between the 1-step and 2-step model appear in this case.

The equation that gives the time evolution of activity concentration in the dissolved phase, C_d, is:

$$\frac{\partial C_d}{\partial t}+u\frac{\partial C_d}{\partial x}+v\frac{\partial C_d}{\partial y}+w\frac{\partial C_d}{\partial z}=A\left(\frac{\partial^2 C_d}{\partial x^2}+\frac{\partial^2 C_d}{\partial y^2}\right)+\frac{\partial}{\partial z}\left(K\frac{\partial C_d}{\partial z}\right)-\sum_{i=1}^{N}k_{11,i}C_d+k_2\sum_{i=1}^{N}m_i C_{s,i}+\pi\left(k_2\frac{L\rho_s\phi\sum_{i=1}^{N}f_i A_{s,i}}{\Upsilon}-\sum_{i=1}^{N}k_{12,i}C_d\right) \quad (6)$$

where A and K are the horizontal and vertical diffusivities, respectively, and u, v and w are the components of the water velocity in the direction of axes x, y and z. It is considered that A is constant and K changes in both the horizontal and vertical directions. It is computed from the turbulence model. $C_{s,i}$ and $A_{s,i}$ are, respectively, the concentration of radionuclides in suspended matter and bottom sediments of class i and ρ_s is the sediment bulk density. We set $\pi = 0$ unless we are solving the equation for the water layer in contact with the sediment. In this case $\pi = 1$ to allow interactions between water and sediments.

The equation that gives the time evolution of activity concentration in each of the suspended matter classes is:

$$\frac{\partial(m_i C_{s,i})}{\partial t}+u\frac{\partial(m_i C_{s,i})}{\partial x}+v\frac{\partial(m_i C_{s,i})}{\partial y}+(w-w_{s,i})\frac{\partial(m_i C_{s,i})}{\partial z}=A\left(\frac{\partial^2(m_i C_{s,i})}{\partial x^2}+\frac{\partial^2(m_i C_{s,i})}{\partial y^2}\right)+\frac{\partial}{\partial z}\left(K\frac{\partial(m_i C_{s,i})}{\partial z}\right)+k_{11,i}C_d-k_2 m_i C_{s,i}+\pi(-\mathrm{DPR}_i+\mathrm{ERR}_i) \quad (7)$$

where $w_{s,i}$ is particle settling velocity, π has the same meaning as above and DPR_i is the deposition of radionuclides from the deepest water layer to the sediment evaluated according to:

$$\mathrm{DPR}_i=\frac{w_{s,i}m_i(b)C_{s,i}(b)}{\Upsilon}\left(1-\frac{\tau_b}{\tau_{cd}}\right) \quad (8)$$

Note that (b) means that the corresponding magnitude is evaluated at the deepest water layer. ERR_i is the resuspension of radionuclides due to sediment

erosion:

$$\mathrm{ERR}_i = \frac{Ef_i A_{s,i}}{\Upsilon}\left(\frac{\tau_b}{\tau_{ce}} - 1\right) \tag{9}$$

In these equations E is the erodability constant, τ_b is bed stress and τ_{cd} and τ_{ce} are critical deposition and erosion stresses, respectively. Of course, deposition of radionuclides is calculated only if $\tau_b < \tau_{cd}$ and resuspension only if $\tau_b > \tau_{ce}$. Activity concentration in the total suspended phase is calculated as:

$$C_s^{\mathrm{total}} = \frac{\sum_{i=1}^{N} m_i C_{s,i}}{\sum_{i=1}^{N} m_i} \tag{10}$$

The equation for the temporal evolution of specific activity in each bed sediment particle class is:

$$\frac{\partial A_{s,i}}{\partial t} = k_{12,i}\frac{C_d \Upsilon}{L\rho_s f_i} - k_2 A_{s,i}\phi + \mathrm{DPR}_i - \mathrm{ERR}_i \tag{11}$$

where it is remembered that $\Upsilon = \Delta z$ and the deposition and erosion terms are calculated as:

$$\mathrm{DPR}_i = \frac{w_{s,i} m_i(b) C_{s,i}(b)}{L\rho_s f_i}\left(1 - \frac{\tau_b}{\tau_{cd}}\right) \tag{12}$$

$$\mathrm{ERR}_i = \frac{EA_{s,i}}{L\rho_s}\left(\frac{\tau_b}{\tau_{ce}} - 1\right) \tag{13}$$

Total specific activity in bed sediments is calculated from specific activity in each particle class:

$$A_s^{\mathrm{total}} = \sum_{i=1}^{N} f_i A_{s,i} \tag{14}$$

2.3. Numerical solution

All the equations are solved using explicit finite difference schemes. The scheme described in Flather and Heaps (1975) is used to solve the hydrodynamic equations. Radiation conditions are applied along open boundaries. The MSOU second order scheme (Vested et al., 1996) is used to solve the advection terms in all the dispersion equations (salinity, suspended matter, radionuclides) and a second order scheme (Kowalick and Murty, 1993) is also used for the diffusion terms.

The hydrodynamic calculations are started from rest and an uniform salinity of 38 g/l is assumed. The effect of the large-scale circulation is neglected in the area under study, as done by Marsaleix et al. (1998), as well as tidal currents, that are practically nonexisting (Marsaleix et al., 1998; Tsimplis et al., 1995). Indeed, M_2 currents are below 1 cm/s in most parts of the Mediterranean and S_2 currents have smaller amplitudes.

Open boundary conditions must also be given for suspended matter particles and radionuclides. The open boundary condition described in Periáñez (1999) and Periáñez (2000) has been adopted:

$$C_i = \psi C_{i-1} \tag{15}$$

where C_i represents the concentration of suspended matter and radionuclides outside the computational domain and C_{i-1} represents the concentration just inside it. The nondimensional value of ψ is obtained from a calibration exercise.

The hydrodynamic model is run for a given water discharge from the Rhone until a steady salinity and current amplitude pattern is obtained. Then, the suspended matter model is run using such water circulation. The suspended matter model (without the erosion term) is started from a sea bottom containing no sediments. Then, the accumulation of particles of each class is calculated to have a first estimation of the distribution of sediment classes over the model domain. Next, the suspended matter model is started (with erosion) from the estimated distribution of particle classes until a steady state is reached. This way a self-consistent distribution of different particle classes on the sea bed over the model domain can be obtained. This distribution is relevant to calculate the adsorption of radionuclides by the bed sediments since they adsorb radionuclides from the deepest part of the water column.

Once the water circulation, salinity distribution, suspended matter distribution for each particle class and distribution of particles in bed sediments are known and stored in files, the radionuclide dispersion model may be run using these files as input data.

The model domain is presented in Fig. 1. The model resolution is $\Delta x = \Delta y = 1000$ m. A variable grid is used in vertical to have enough resolution to

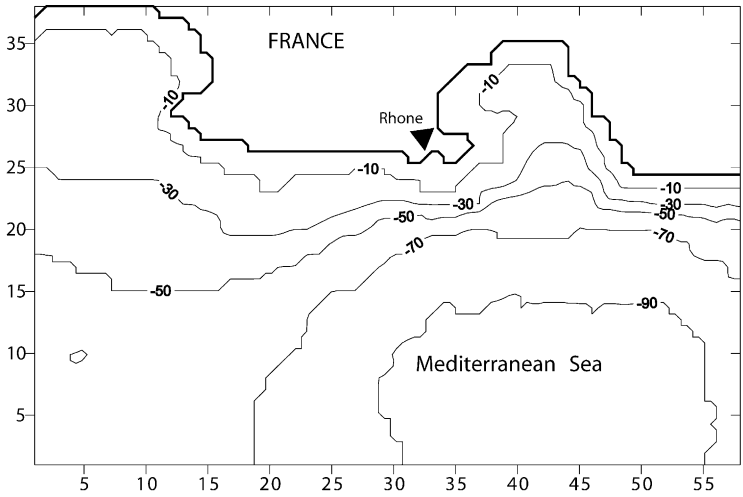

Fig. 1. Model domain. Each unit in the x and y axis is 1000 m. Depths are given in m.

solve the salinity gradients in the surface plume. Thus, 10 layers with $\Delta z = 1$ m are used followed by thicker layers increasing to $\Delta z = 15$ m. Time step is fixed as 5 s to solve the hydrodynamic equations due to the CFL stability condition. It is increased to 60 s to solve the suspended matter and radionuclide equations. However, when the radionuclide dispersion model was applied to plutonium, the time step had to be decreased to 10 s since the following stability condition is introduced by the terms describing the transfers between the liquid and the solid phases:

$$\Delta t < \frac{1}{k_{\max}} \tag{16}$$

where $k_{\max}$ is the maximum kinetic rate involved in the equations. It means that the activity transferred from one phase to another in a time step must be smaller than the activity content in the origin phase. This condition is more restrictive for a highly reactive radionuclide as Pu than for more conservative ones as, for instance, Cs.

2.4. *Parameters for the model*

Values to the different parameters in the model must be given, as well as the appropriate source term for suspended matter particles and radionuclides.

The average discharge from the Rhone River is 1700 m^3/s (Broche et al., 1998; Thill et al., 2001). Wind conditions affect the extension and shape of the plume (Estournel et al., 1997, 2001). Two types of winds are predominant in the region: northwest winds (representing 45% of winds exceeding 10 m/s on average over the year) and southeast winds (20% of winds exceeding 10 m/s). The plume response to winds has been studied in the references given above. Although wind stress is formally included in the hydrodynamic equations, the main difficulty in the present work is that observed sedimentation rates, the distribution of different particle classes over the bed and measured activity concentrations in bed sediments integrate many different wind and river discharge conditions. On the other hand, measured activity concentrations in the water column correspond to the particular conditions during sampling, that, on the other hand, took place over a period of several months (Martin and Thomas, 1990). As a consequence, it was decided to run the hydrodynamic model for average discharge from the Rhone River and without wind. This may be a too simple approach, but can give a realistic view of the main dispersion processes in the plume, given the generally good agreement between measured and computed activity concentrations. Nevertheless, the sensitivity of radionuclide transport in the plume to changing winds is an interesting problem that has to be addressed in the near future since dispersion processes related to meteorological conditions may become apparent.

The computed water circulation and salinity distribution are stored in files that will be used to calculate the suspended matter distribution, sedimentation rates and the distribution of particles over the sea bed.

The average suspended matter discharge of the Rhone River is about 4.6 Mt/year (Thomas, 1997), although a value of about 7.6 Mt/year has been more recently reported (Antonelly, 2002). The annual discharge fluctuates between 2.6

and 26.5 Mt (Antonelly, 2002) since it has a relevant variability, with most of the solids being discharged during flood events. Thomas (1997) has established a correlation for the suspended matter concentration in the river vs. water flow. If such correlation is applied to the average water discharge (1700 m^3/s), a suspended matter concentration in the river of 28 mg/l is obtained. This will be the suspended matter source term used in the model. This estimation is in agreement with measurements. For instance, Garnier et al. (1991) measured a suspended load of 17.6 mg/l for a water discharge of 1600 m^3/s; Martin and Thomas (1990) measured 11.3 and 54.0 mg/l for water discharges of 1300 and 2200 m^3/s, respectively and Eyrolle et al. (2002) obtained a suspended load of 28.6 mg/l for a water discharge of 1718 m^3/s.

Four suspended matter particle classes are considered in the model. Thill et al. (2001) measured the proportion of particles of five different classes for low, average and high water discharges. From the total particle concentration given above (28 mg/l) and the proportion of particles of each class (for average water discharge), the particle concentration for each class can be calculated. Results are given in Table 1. These concentrations are the boundary conditions of the suspended matter model at the river mouth. The largest particle class measured by Thill et al. (2001) has been neglected due to the extremely low proportion in which such particles are present (0.014% of the total). Settling velocities obtained from Stokes's law (applied to the average particle size of each class) are also given in Table 1. It is possible to include flocculation processes in the settling velocity using the typical relation shown, for instance, in Tattersall et al. (2003). However, it is not done since Thill et al. (2001) found a poor reactivity of suspended matter of the area regarding salt induced flocculation. Colloidal aggregation is not considered in the model (the reasons why colloids are neglected are given below).

The threshold deposition stress has been fixed as 0.1 N/m^2. This parameter has been observed to be in the range 0.06–1.1 N/m^2 (Krone, 1962; Mehta and Partheniades, 1975). After some preliminary calculations without wind, it was found that results were not affected by the erosion term. However, erosion events may be induced by wind waves in the shallower areas. Indeed, waves are the main factor producing sediment erosion in the region (REMOTRANS, 2004). Nevertheless, wave-induced erosion is not included in the model since calculations are carried out under calm conditions (the models of Estournel et al. (1997) and Kondrachoff

Table 1
Average particle size for each particle class included in the model and their corresponding settling velocities. The particle concentration at the Rhone River mouth for average water discharge is also given

Average particle size (μm)	w_s(m/s)	m (mg/l)
3	7.8×10^{-6}	11.5
7	4.2×10^{-5}	9.5
20	3.5×10^{-4}	3.5
40	1.4×10^{-3}	3.5
Total load		28

et al. (1994) do not include sediment erosion although do consider winds). The suspended matter model also provides the distribution of the different particle classes on the sea bed over the model domain (parameter f_i for each particle class), as well as provides sedimentation rates over the domain, that can be compared with those derived from observations.

Radionuclides used in the simulations are ^{137}Cs and ^{239,240}Pu. Values for the kinetic coefficients have to be defined. The exchange velocity depends on water salinity through Eq. (4). The 50% saturation salinity is obtained from the experiments in Laissaoui et al. (1998): $S_0 = 45$ g/l. As described in Nyffeler et al. (1984) and also found in the experiments of Laissaoui et al. (1998), k_2 is very similar even for radionuclides with a rather different geochemical behaviour and it does not seem to be affected by salinity. Thus, the value given to k_2 is the same that was used in the plutonium dispersion model of the Irish Sea (Periáñez, 1999): $k_2 = 1.16 \times 10^{-5}$ s^{-1}. The freshwater value for the exchange velocity has been obtained from the equation relating this parameter with k_2 and the freshwater distribution coefficient, k_{d}^0 (Periáñez et al., 1996a):

$$k_{\mathrm{d}}^0 = \frac{\chi_1^0}{k_2}\frac{3}{\rho \bar{R}} \tag{17}$$

where $\bar{R}$ is the mean radius of suspended matter particles in the river, that has been calculated from the proportion of particles of each class in the river given in Thill et al. (2001).

The behaviour of Pu in aquatic systems is of considerable complexity due to the fact that it can exist in different oxidation states simultaneously. The reduced Pu [Pu(III) and Pu(IV)] is highly particle reactive and has been shown to possess a k_{d} that is approximately two orders of magnitude higher than that of the more soluble oxidized Pu [Pu(V) and Pu(VI)]. Different exchange velocities (obtained from the different $k_{\mathrm{d}}^0 s$ through Eq. (17)) should be used for oxidized and reduced Pu, as has been done in Periáñez (2003). However, in this work different plutonium oxidation states have not been considered due to the lack of experimental data on Pu speciation in the Rhone area. Thus, measurements (of Pu concentrations and $k_{\mathrm{d}} s$) represent the mixture of oxidation states that is present in the particular sample. A measured effective k_{d}^0, representative of such mixture, is used to obtain an effective exchange velocity. This approach for simulating Pu dispersion is used in other models (Periáñez, 1999; Aldridge et al., 2003).

The freshwater values of the distribution coefficients for Cs and Pu have been measured in Martin and Thomas (1990). The following freshwater exchanges velocities have been obtained for Cs and Pu, respectively: 3.80×10^{-6} and 5.21×10^{-5} m/s. The sorption of radionuclides onto particles obviously depends on the nature and type of such particles. It must be noted that the exchange velocities are obtained from site-specific distribution coefficients. Thus, the exchange velocities used in the model reflect the nature of particles present in the area.

The sediment mixing depth was fixed as $L = 0.1$ m, as in previous modelling works (Periáñez et al., 1996a; Periáñez, 1999). After a calibration process, the

geometry correction factor is defined as $\phi = 0.1$ and it is used $\psi = 0.99$ in open boundary condition (Eq. (15)). Particles transported by the river have a typical density $\rho = 2600$ kg/m^3 (Arnoux-Chiavassa, 1998) and dry density of bed sediments is fixed as $\rho_s = 1600$ kg/m^3 (Zuo et al., 1997).

The input of radionuclides from the river has also been obtained from Martin and Thomas (1990), who estimated the radionuclide input to the Mediterranean in dissolved and particulate forms. The input of radionuclides fixed to suspended particles is distributed among the four particle classes according to the distribution coefficient for each class. This distribution coefficient is calculated by Eq. (17) but replacing $\bar{R}$ by the corresponding average particle radius R_i of each class. Inputs from the river have been obtained from sampling campaigns carried out in the period 1982–1985. For this time the main source of radionuclides to the river is due to the discharges from Marcoule reprocessing plant, being fallout and watershed soil leaching negligible if compared with them. Also, no relevant discharge variations have been found in these years (Martin and Thomas, 1990). Although short-term variations cannot be assessed, estimations of the inputs to the Mediterranean carried out in Martin and Thomas (1990) provide a realistic reference for the average flux of radionuclides from the Rhone.

It has been found that Cs is not significantly fixed to colloids (Eyrolle and Charmasson, 2001). The fraction of colloidal Pu measured by Eyrolle and Charmasson (2004) ranges from 0% to 41% of the dissolved phase plutonium content. Considering that over 90% of Pu is fixed to suspended matter (see below), the fraction of colloidal Pu represents a maximum of 4% of the total Pu content. Thus, colloids have been neglected in the case of Pu as well. Also, it seems that changes in POC (particulate organic carbon) do not affect significantly the adsorption of radionuclides (Thomas, 1997).

The dispersion of radionuclides released from the river is calculated until a steady distribution is obtained. The radionuclide discharges are carried out assuming that the sea is initially not contaminated.

3. Results and discussion

The computed currents and salinity distribution are in agreement with the earlier calculations of Estournel et al. (1997), Marsaleix et al. (1998) and Arnoux-Chiavassa (1998). Broche et al. (1998) released a surface drifter 2 km south from the river mouth and measured its langrangian velocity during several hours. The movement of a surface drifter has been simulated with the model for the same conditions of the experiment in Broche et al. (1998), water discharge equal to 2000 m^3/s and no wind. A comparison between the observed and computed lagrangian velocity of the drifter is presented in Fig. 2. It can be seen that there is a good agreement between both sets of data, indicating that the model is giving a realistic representation of currents in the Rhone plume. The shape of the salinity contours and currents indicate that the plume forms a bulge of anticyclonic circulation in front of the river mouth. The circulation in the plume is baroclinic, that is, induced by the density differences.

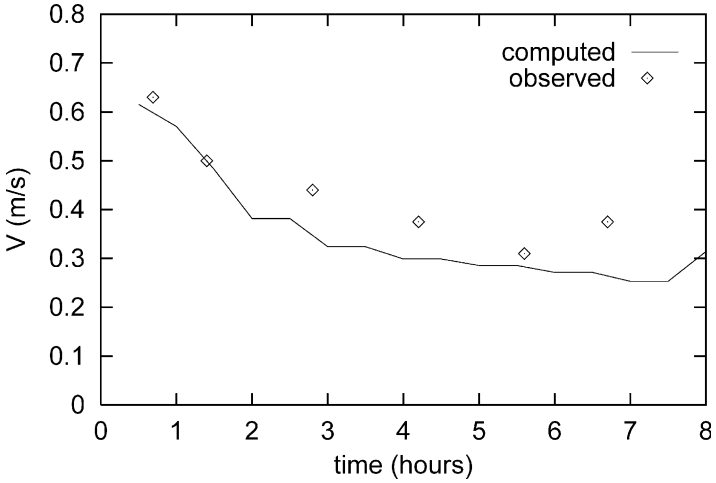

Fig. 2. Observed (Broche et al., 1998) and computed lagrangian velocities of a surface drifter released 2 km south from the river mouth.

A map showing the total concentration of particles obtained after a computation time of 3 days can be seen in Fig. 3a. The shape and extension of the plume is in agreement with that obtained from satellite observations (Kondrachoff et al., 1994). The plume is directed to the southwest offshore, following the water circulation. It is mainly composed of fine sediments, as the coarser fractions sink close to the river mouth. This can be clearly seen with the help of Fig. 3b: coarse particles (20 and 40 μm average sizes) soon disappear from the water column as they sink to the sea bed. The largest particles are entirely removed from the water col-

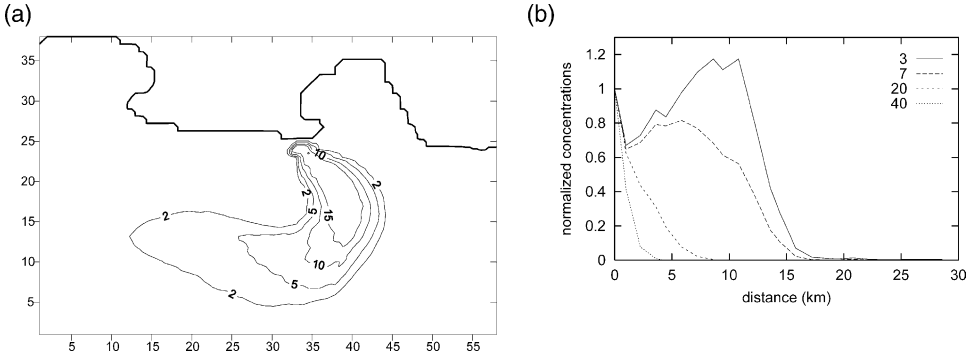

Fig. 3. (a) Computed total suspended matter concentrations (ppm) over the model domain at the surface after a computation time of 3 days. (b) Computed surface suspended matter concentrations for each particle class along the axis of the plume normalized to the concentrations in the river mouth. Particle classes are characterized by their average sizes (given in μm). Distances are measured with respect to the river mouth.

umn in less than 5 km, as found by the observations in Thill et al. (2001). The content in particle class characterized by an average size of 7 μm decreases to 50% in 10 km, which is similar to the distance of 8 km found in Thill et al. (2001). It can be observed that the content in the smallest particles (3 μm average size) initially increases, before being finally reduced as the plume is diluted. This increase in surface concentrations of the smallest particles has also been observed in Thill et al. (2001). Several hypothesis were proposed to explain it, like larger particle break-up, primary production, colloid aggregation or simple mixing with a particle-rich saline water source, although none of these mechanisms could clearly explain the behaviour of the smallest particles. It seems, however, that the particle increase is a hydrodynamic effect since any other process has not been included in the model.

The computed sedimentation rates along the plume axis are shown in Fig. 4 together with the estimations presented in Radakovitch et al. (1999) obtained from ^{210}Pb profiles. The model underestimates the sedimentation rates. However, the following points have to be considered: first, sedimentation rates estimated from observations are maximum possible values since they are calculated assuming that there is no diffusion in the sediment core. Second, the values obtained from the model are calculated for an average water discharge, and sedimentation increases after flood events when a large amount of suspended matter is discharged by the river. Finally, if must be taken into account that bed-load transport of coarse material is not included in the model. This process can also contribute to a larger sedimentation rate.

Nevertheless, the model gives a realistic representation of the sedimentation process in the plume. Computed sedimentation rates are similar to those derived by several authors from observations (Radakovitch et al., 1999; Zuo et al., 1997; Charmasson et al., 1998): a deposition belt is observed close to the river mouth, where sedimentation reaches values of the order of 10 cm/year, decreasing to

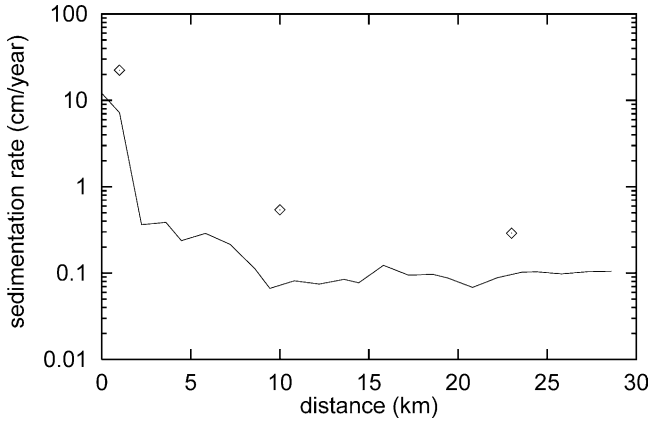

Fig. 4. Computed sedimentation rates along the plume (line) together with the values estimated from observations (Radakovitch et al., (1999). Distances are measured with respect to the river mouth.

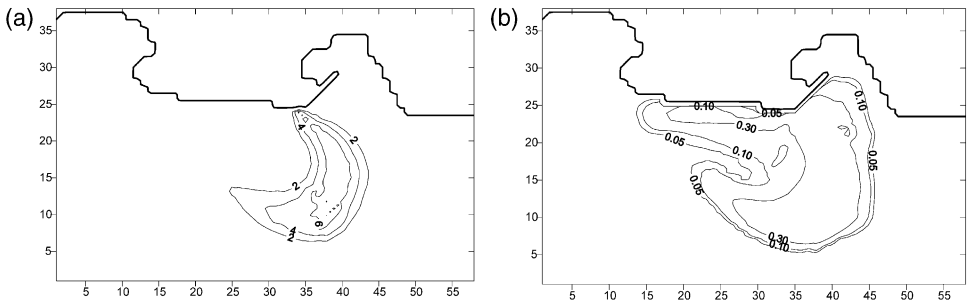

Fig. 5. Computed distributions of ^{137}Cs in surface water (a), Bq/m^3, and suspended matter (b), Bq/g, due to discharges from the river.

values of the order of 10^{-1} cm/year as moving away from the mouth. Maps showing the distribution of particles of different classes over the bed, as well as sedimentation rates for each particle class over the model domain can also be obtained.

The computed distribution of ^{137}Cs in water and suspended matter due to discharges from the river is presented in Fig. 5. The dissolved pattern closely follows the water circulation in the plume, but a different distribution is found for radionuclides fixed to suspended particles: in this case activity is also transported towards the west along the coast. Model results are compared with observations in Fig. 6, where south–north profiles in front of the river mouth of ^{137}Cs in surface

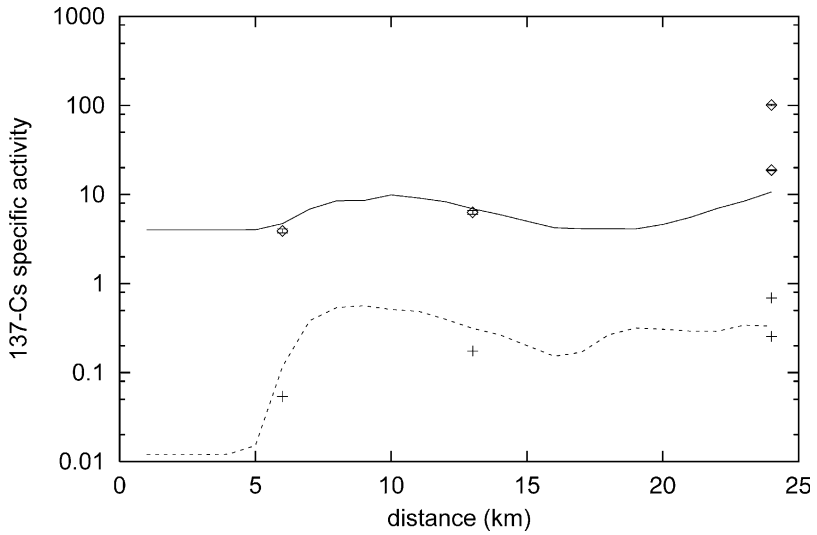

Fig. 6. Measured (points) and computed (lines) south–north profiles of ^{137}Cs in surface water (solid line, boxes), in Bq/m^3, and suspended matter (dashed line, crosses), in Bq/g, in front of the river mouth. Distances are measured form the south of the model domain (the river mouth is at km 24). Measurements are taken from Martin and Thomas (1990).

water and suspended matter are shown. Measured activity levels correspond to the addition of discharges from the river and fallout over the Mediterranean. An uniform activity background, due to atmospheric fallout, has been added to the computed specific activities (given in Fig. 5, which correspond to the input from the river) in order to compare model results with observations. Pre-Chernobyl ^{137}Cs specific activities due to fallout in the Mediterranean range from 3.1 (Martin and Thomas, 1990) to 5.4 Bq/m^3 (Gascó et al., 2002). An intermediate value of 4 Bq/m^3 has been used for the dissolved background. From this quantity, and assuming that the distribution of fallout radionuclides between water and suspended particles is at equilibrium, the fallout background in suspended matter is calculated using the equilibrium k_d of 3×10^3 l/kg given in IAEA (1985). Its value is 0.012 Bq/g. It can be seen in Fig. 6 that the model gives a good representation of activity levels detected in the river plume in both dissolved and particulate forms.

The computed distribution of ^{137}Cs in bed sediments is presented in Fig. 7, together with observations obtained from Martin and Thomas (1990). It can be seen that the model gives a correct estimation of activity levels in the vicinity of the river mouth, although it underestimates them away from the river mouth. It must be taken into account that sediments integrate radionuclide input variations over time. Also, episodes of high river discharge, when larger amounts of particles are released to the sea and are also transported to greater distances from the river mouth, as well as different wind conditions, are integrated in the measured concentrations. Computed concentrations are obtained for average water, suspended particles and radionuclide discharges. It is not possible to have a accurate agreement between measurements and computations with a model working in *average*

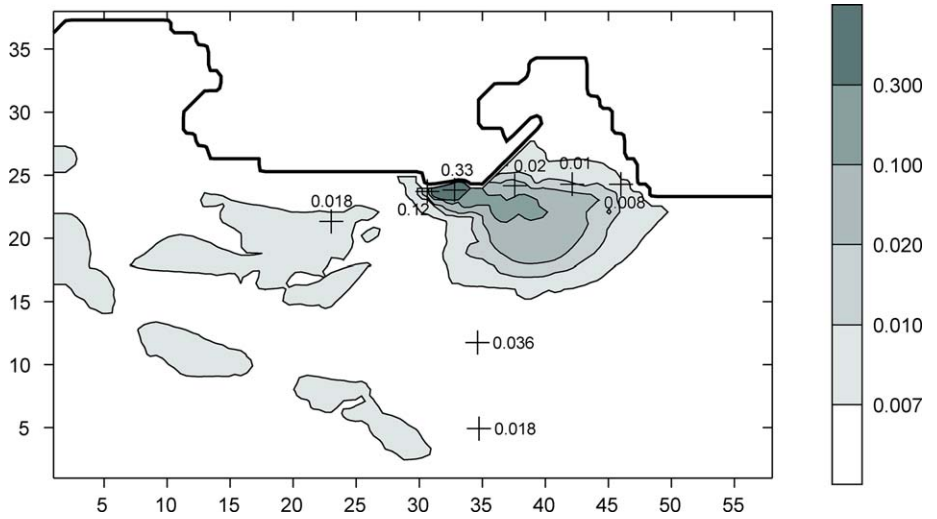

Fig. 7. Computed distribution of ^{137}Cs in bed sediments (Bq/g). Measured concentrations (Martin and Thomas, 1990) are also shown.

conditions. Nevertheless, it seems clear that the model produces rather realistic activity levels in the area of the river mouth. Indeed, the distribution map in Fig. 7 is very similar to that presented in Charmasson (2003), where a sharp decrease in inventories with distance from the river mouth can be seen. Finally, it must be taken into account that measured bed concentrations include deposition from global fallout. Only sampling stations close to the river mouth in Charmasson (2003) present ^{137}Cs inventories clearly in excess with respect the cumulative deposit due to global fallout (Chernobyl is not considered since it occurred later than the time of our simulations). Thus, most of ^{137}Cs in sediments appears in a well-delimited zone in the close vicinity of the river mouth. Our simulations are in agreement with these findings.

The model can also give a wide amount of information, as fractions of radionuclides in suspended matter (for total suspended load and each particle class) and distribution coefficients for suspended matter–water and bed sediment–water systems (also for the total solid phase and each particle class). It is interesting to point out that the model can calculate distribution coefficients instead of requiring them as input data.

As an example, the computed fraction of ^{137}Cs fixed to suspended matter particles in surface waters of the plume is presented in Fig. 8. It can be seen that about 60% is fixed to solid particles. In Eyrolle and Charmasson (2001), it is pointed out that 30% of ^{137}Cs is transported by the Rhone River in the particulate phase, although this percentage is increased to 83% in Martin and Thomas (1990). Indeed, these authors have found that the particulate phase is the major vector for most of the radionuclides. Calmet and Fernandez (1990) have also found that ^{137}Cs associated with particles represents 68% of the Rhone input. Computed suspended matter–water distribution coefficients (total suspended matter) for surface waters are also presented in Fig. 8. They are of the order of 10^4 l/kg in the area of the plume, decreasing in one order of magnitude out of it and approaching the average value recommended by IAEA (1985) for Cs (3×10^3 l/kg). This behaviour may be similar to that observed (Mitchell et al., 1995) in the Irish Sea for Pu [and also reproduced by a model (Periáñez, 1999)], where distribution coefficients decrease when

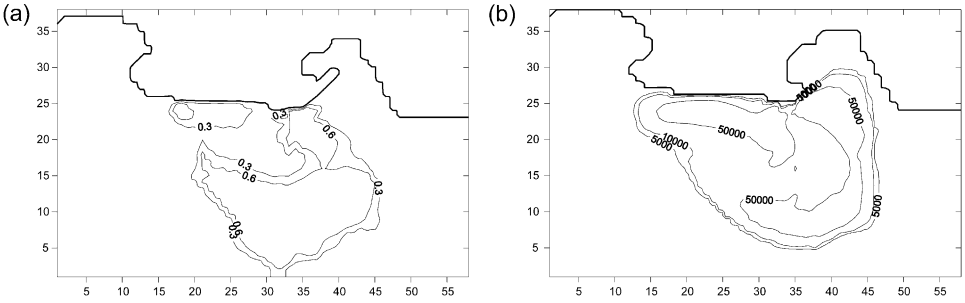

Fig. 8. Computed ^{137}Cs fraction fixed to suspended particles in surface waters (a) and computed suspended matter–water k_d (l/kg) in surface waters (b).

increasing distance from Sellafield. It was attributed to the nature of discharges since virtually all plutonium was released in particulate form. The same situation is presented in the plume since most ^{137}Cs is released in particulate form. However, the decrease in the exchange velocity with salinity included in the model Eq. (4) will also produce a decrease in the distribution coefficients as distance from the river mouth increases and, consequently, salinity increases too.

The dependence of the distribution coefficient with particle size can be seen in Fig. 9. Here, the computed k_d for each particle class in an arbitrary point of the surface plume is presented. It can be seen that $k_d s$ decrease with increasing particle size. Abril and Fraga (1996) obtained an equation for the dependence of distribution coefficients with particle size assuming spherical particles and that only a surface layer, instead of the whole particle, participates in the adsorption process:

$$k_d = \frac{a_s}{a_w}\left[1 - \left(1 - \frac{\xi}{R}\right)^3\right] + \frac{a_c}{a_w}\left(1 - \frac{\xi}{R}\right)^3 \tag{18}$$

where a_w is specific activity in water, a_s and a_c are specific activities in the surface layer and central part of particles, respectively, and ξ is the thickness of the surface layer. If it is considered that man-made radionuclides are generally fixed to the surface layer of mineral particles, neglecting hot particles, then $a_c = 0$ (Abril and Fraga, 1996) and:

$$k_d = \frac{a_s}{a_w}\left[1 - \left(1 - \frac{\xi}{R}\right)^3\right] \tag{19}$$

This equation indicates that k_d decreases with particle radius. Computed $k_d s$ have been fitted to a function of this form (solid line in Fig. 9) for an arbitrary

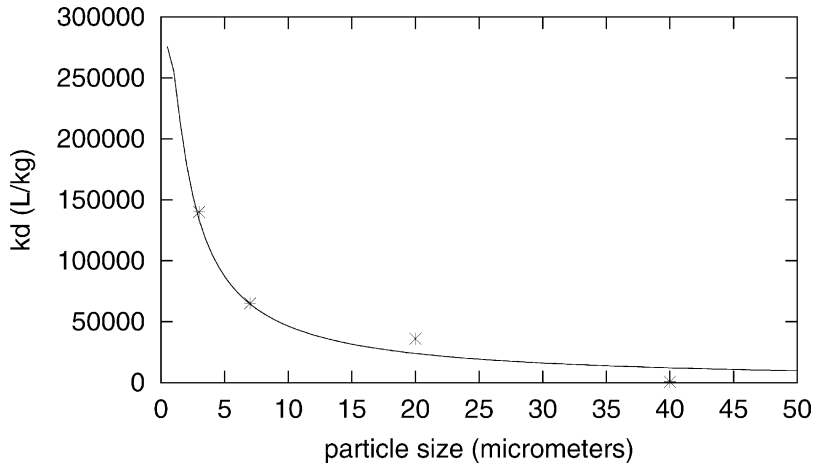

Fig. 9. Computed ^{137}Cs distribution coefficients (l/kg) for the average particle size (μm) of each class at an arbitrary point of the plume and numerical fitting to Eq. (19). (line).

point inside the plume. From this fitting, $\xi = 0.6 \pm 0.8$ μm. Abril and Fraga (1996) deduced, from observations, a value equal to 1.9 μm. Thus, the model gives the theoretically predicted behaviour of distribution coefficients and the thickness of the exchange layer has been estimated. This number can be compared with the value deduced by Abril and Fraga (1996) from observations. Although the model result is presented for only one point, the behaviour of k_ds is the same over all the plume, and the same values, within numerical fitting errors, are obtained for ξ.

South–north vertical profiles of activity concentrations in suspended matter in front of the river mouth and for several particle classes are presented in Fig. 10, together with specific activity in total suspended load. It can be seen that the radionuclide content in the plume suspended load is essentially controlled by the smallest particles, since Figs. 10a and 10b are very similar. Coarse particles quickly sink to the bottom and, as a consequence, radionuclides are only present in a small region in front of the river mouth as can be seen in Figs. 10c and 10d. This is in

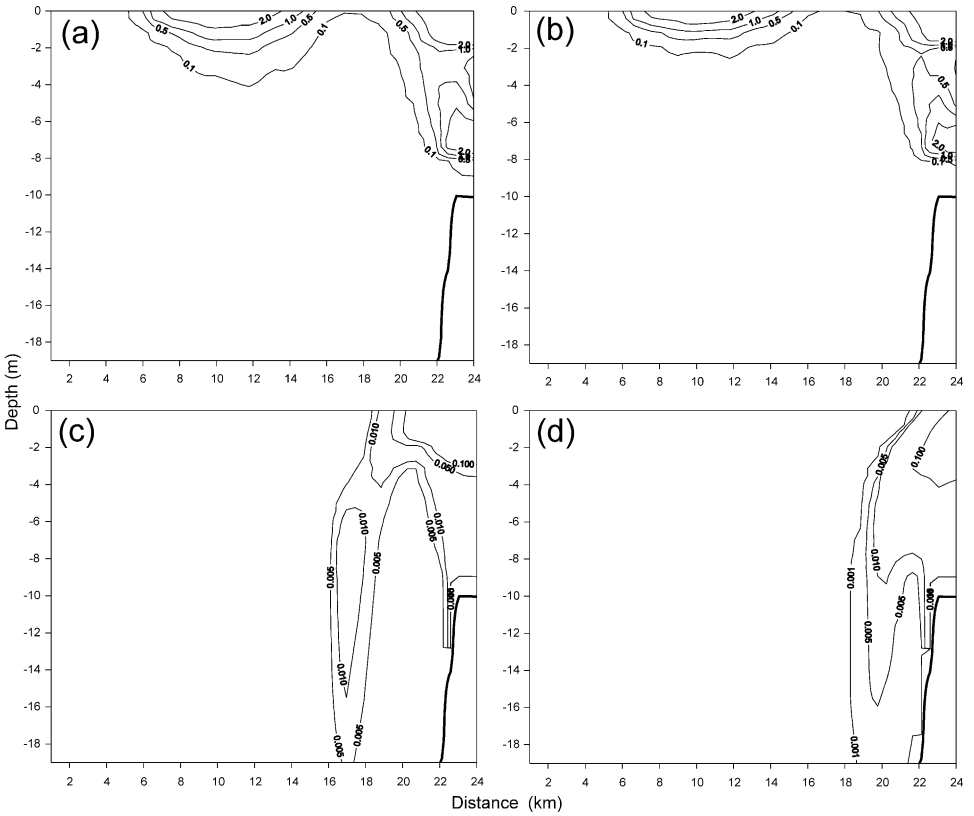

Fig. 10. Computed ^{137}Cs activity in suspended matter in Bq/m^3 for a south–north vertical profile in front of the river mouth. (a) total suspended matter. (b), (c) and (d) 3, 20 and 40 μm particles, respectively. Distances are measured from the south of the model domain. The river mouth is at km 24.

agreement with the results of Martin and Thomas (1990), who found a deposition belt close to the river mouth. It seems that this deposition belt is produced by the coarsest particles in the plume.

Calmet and Fernandez (1990) have measured a decrease in ^{137}Cs activity with increasing depth in the water column. Such decrease has also been produced by the model although numbers cannot be directly compared since measurements include the input of radionuclides from the Rhone plus Chernobyl fallout and the model does not account for the last.

A comparison of model results with measurements for the application to ^{239,240}Pu is presented in Fig. 11, where south–north plutonium profiles in water and suspended matter in front of the river mouth are shown. Plutonium fallout backgrounds have been added to the activity concentrations calculated by the model, which correspond to the input from the river only. Specific activity in water due to fallout plutonium is 0.016 Bq/m^3 (Martin and Thomas, 1990). Using the Pu k_d value measured in the northwestern Mediterranean (Molero et al., 1995), 1.4×10^5 l/kg, which is also in good agreement with the average value of the Pu distribution coefficient in coastal waters recognized in IAEA (1985), 1.0×10^5 l/kg, the specific activity in suspended matter particles due to fallout plutonium (again assuming equilibrium for fallout radionuclides) is 0.0024 Bq/g. It can be seen that the model gives a correct estimation of plutonium levels in both phases in the river plume. These activity levels are two orders of magnitude lower than those of ^{137}Cs due to the smaller Pu input rate. The fraction of plutonium at the surface fixed to the suspended particulate phase is given in Fig. 12. It can be seen that over 90% of Pu in the plume is attached to particles. This is in agreement with Thomas (1997), who found that plutonium predominates in particulate form in most hydrological

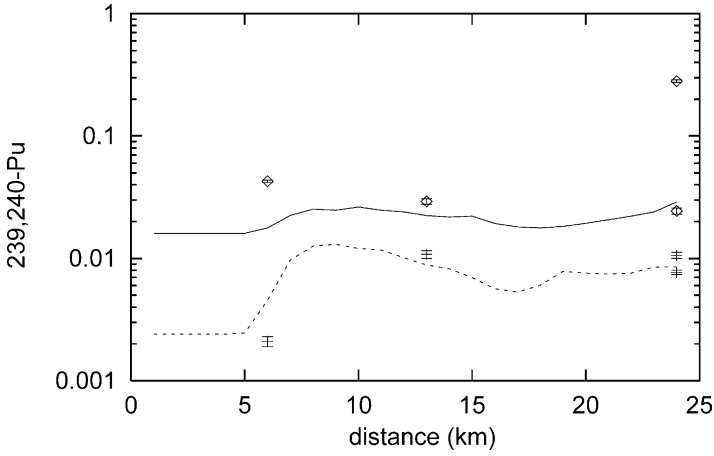

Fig. 11. Measured (points) and computed (lines) south–north profiles of ^{239,240}Pu in surface water (solid line, boxes), in Bq/m^3, and suspended matter (dashed line, crosses), in Bq/g, in front of the river mouth. Distances are measured from the south of the model domain (the river mouth is at km 24). Measurements are taken from Martin and Thomas (1990).

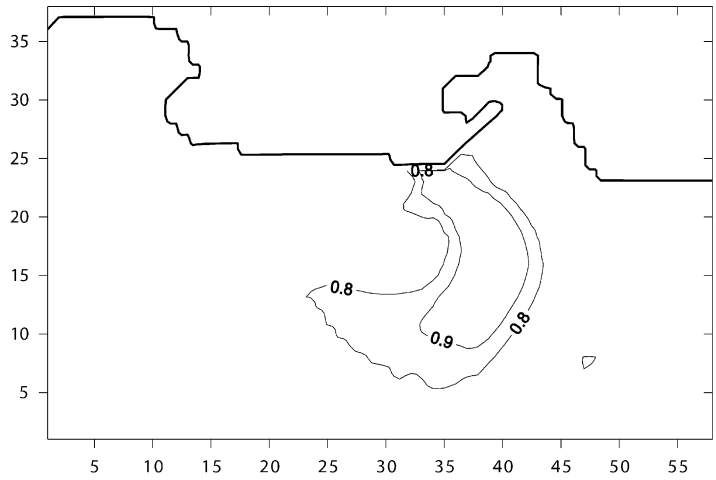

Fig. 12. Computed ^{239,240}Pu fraction fixed to suspended particles in surface waters.

conditions and with Eyrolle and Charmasson (2004), who have reported that 85% of Pu isotopes are bound to particles in the river. Computed distribution coefficients in the plume are of the order of 3×10^5 l/kg, decreasing out of it and approaching the value found by Molero et al. (1995).

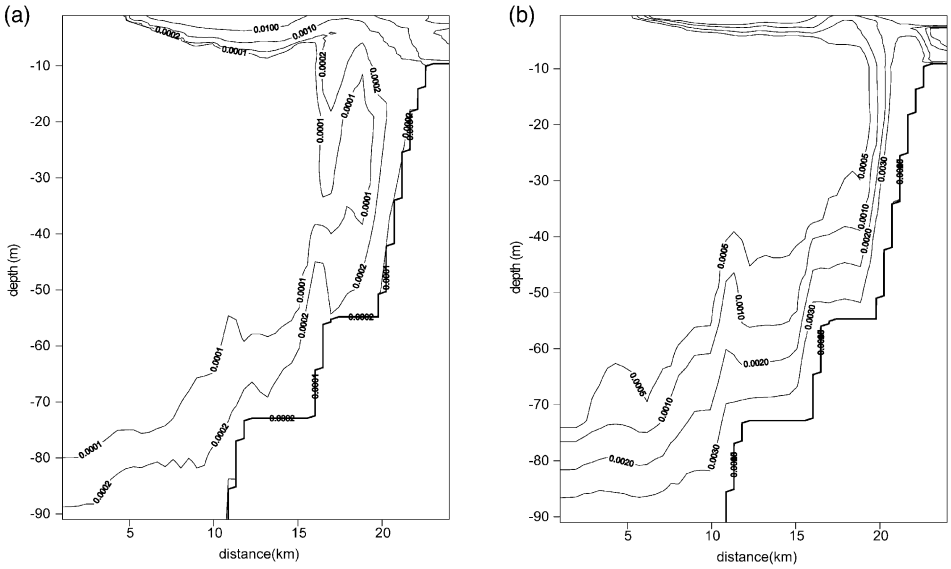

Fig. 13. Computed ^{239,240}Pu activity in suspended matter (a) and water (b), both in Bq/m^3, for a south–north vertical profile in front of the river mouth and for total suspended matter.

Vertical profiles, in front of the river mouth, of plutonium in water and total suspended matter (both in Bq/m^3), can be seen in Fig. 13. The suspended matter profile is clearly different to that of ^{137}Cs (Fig. 10a). In this case, it can be appreciated, together with the surface plume, a deep layer with some Pu content which appears due to the higher reactivity of plutonium. This deep layer is composed of the coarse particles that sink quickly after they are released from the river. When these contaminated particles penetrate the bottom waters (not contaminated by Pu discharged from the Rhone), plutonium is partially redissolved. This leads to the sub-surface layer of contaminated water that can be seen in Fig. 13b. Indeed, Eyrolle and Charmasson, (2004) have detected some Pu coming from Marcoule discharges in the bottom waters of the mixing zone.

4. Conclusions

A full 3D model has been developed to simulate the transport of radionuclides in the Rhone River plume. Currents are mainly baroclinic (induced by water density differences). Thus, the hydrodynamic model must include the terms accounting for such density differences in the equations and must also have a vertical resolution high enough to solve the pycnocline. A turbulence model has also been coupled to provide the vertical eddy viscosity.

Together with the hydrodynamic equations, the model solves the suspended matter dynamics. Several suspended particle classes have been included, since model output is rather sensitive to this parameter and the size spectra of particles discharged by the river is wide. The effect of salinity on uptake kinetics has finally been included. The model provides a wide amount of information, as horizontal distributions and vertical profiles of specific activities in water, total suspended matter and each suspended particle class, percentages of radionuclides in total suspended matter and each particle class, distribution coefficients for total suspended matter and each particle class and distribution of radionuclides in bed sediments, for the total sediment and each particle class.

The model has been applied to simulate the transport of ^{137}Cs and $^{239,240}Pu$ in the plume. The computed water circulation and salinity pattern is, in general, in agreement with observations and earlier hydrodynamic models. The model gives a realistic representation of the behaviour of the different particle classes in the plume, as well as of the sedimentation processes. Model results for radionuclide dispersion are, in general, in good agreement with observations. The model produces realistic activity levels in the dissolved phase, suspended matter and bed sediments, as well as gives a fractionation of radionuclides between the dissolved and solid phases that is in agreement with observations. Finally, vertical profiles of ^{137}Cs and $^{239,240}Pu$ have been obtained. In the case of Cs, a decrease in activity with increasing depth in the water column has been obtained. In contrast, a deep water layer contaminated with Pu coming from the river is produced by the model. These results are also in agreement with observations in the area. Thus, it seems that the processes included in the model have been adequately described.

Acknowledgements

Work supported by ENRESA and EU 5th Framework Programme (1998–2002) Nuclear Fission and Radiation Protection Contract FIGE-CT-2000-00085.

References

Abril, J.M., Fraga, E., 1996. Some physical and chemical features of the variability of k_d distribution coefficients for radionuclides. Journal of Environmental Radioactivity 30, 253–270.

Aldridge, J.N., Kershaw, P., Brown, J., McCubbin, D., Leonard, K.S., Young, E.F., 2003. Transport of plutonium ($^{239/240}$Pu) and caesium (^{137}Cs) in the Irish Sea: comparison between observations and results from sediment and contaminant transport modelling. Continental Shelf Research 23, 869–899.

Antonelly, C. 2002. Flux sedimentaires et morphogenese recente dans le chenal du Rhone aval. PhD thesis, University Aix-Marseille I.

Arnoux-Chiavassa, S., 1998. Modelisation d'ecoulements cotiers stratifies presentant des fronts: application au panache du Rhone. PhD thesis, University of Toulon.

Broche, P., Devenon, J.L., Forget, P., Maistre, J.J., Naudin, J.J., Cauwet, G., 1998. Experimental study of the Rhone plume. Part 1: physics and dynamics. Oceanologica Acta 21, 725–738.

Calmet, D., Fernandez, J.M., 1990. Caesium distribution in northwest Mediterranean seawater, suspended particles and sediments. Continental Shelf Research 10, 895–913.

Cancino, L., Neves, R., 1999. Hydrodynamic and sediment suspension modelling in estuarine systems. Part I: description of the numerical models. Journal of Marine Systems 22, 105–116.

Clarke, S., Elliott, A.J., 1998. Modelling suspended sediment concentrations in the Firth of Forth. Estuarine, Coastal and Shelf Science 47, 235–250.

Charmasson, S., 2003. ^{137}Cs inventory in sediment near the Rhone mouth: role played by different sources. Oceanologica Acta 26, 435–441.

Charmasson, S., Bouisset, P., Radakovitch, O., Pruchon, A.S., Arnaud, M., 1998. Long core profiles of ^{137}Cs, ^{134}Cs, ^{60}Co and ^{210}Pb in sediment near the Rhone River (northwestern Mediterranean Sea). Estuaries 21, 367–378.

Davies, A., Hall, P., 2000. A three dimensional model of diurnal and semidiurnal tides and tidal mixing in the North Channel of the Irish Sea. Journal of Geophysical Research 105, 17079–17104.

Duursma, E.K., Carroll, J., 1996. Environmental Compartments. Springer, Berlin.

Estournel, C., Kondrachoff, V., Marsaleix, P., Vehil, R., 1997. The plume of the Rhone: numerical simulation and remote sensing. Continental Shelf Research 17, 899–924.

Estournel, C., Broche, P., Marsaleix, P., Deveneon, J.L., Auclair, F., Vehil, R., 2001. The Rhone River plume in unsteady conditions: numerical and experimental results. Estuarine, Coastal and Shelf Science 53, 25–38.

Eyrolle, F., Arnaud, M., Duffa, C., Renaud, P., 2002. Plutonium fluxes from the Rhone River to the Mediterranean Sea. Radioprotection Colloques 37, 87–92.

Eyrolle, F., Charmasson, S., 2001. Distribution of organic carbon, selected stable elements and artificial radionuclides among dissolved, colloidal and particulate phases in the Rhone River (France): preliminary results. Journal of Environmental Radioactivity 55, 145–155.

Eyrolle, F., Charmasson, S., 2004. Importance of colloids in the transport within the dissolved phase (<450 nm) of artificial radionuclides from the Rhone River towards the Gulf of Lions (Mediterranean Sea). Journal of Environmental Radioactivity 72, 273–286.

Flather, R.A., Heaps, N.S., 1975. Tidal computations for Morecambe Bay. Geophysical Journal of the Royal Astronomical Society 42, 489–517.

Garnier, J.M., Martin, J.M., Mouchel, J.M., Thomas, A.J., 1991. Surface reactivity of the Rhone suspended matter and relation with trace element sorption. Marine Chemistry 36, 267–289.

Gascó, C., Antón, M.P., Delfanti, R., González, A.M., Meral, J., Pappuci, C., 2002. Variation of the activity concentrations and fluxes of natural (^{210}Po, ^{210}Pb) and anthropogenic radionuclides (^{239,240}Pu, ^{137}Cs) in the Strait of Gibraltar (Spain). Journal of Environmental Radioactivity 62, 241–262.

Goshawk, J.A., Clarke, S., Smith, C.N., McDonald, P., 2003. MEAD (Part 1)-a mathematical model of the long-term dispersion of radioactivity in shelf sea environments. Journal of Environmental Radioactivity 68, 115–135.

Holt, J.T., James, I.D., 1999. A simulation of the southern North Sea in comparison with measurements from the North Sea Project. Part 2: suspended particulate matter. Continental Shelf Research 19, 1617–1642.

IAEA 1985. Sediment k_d and concentration factors for radionuclides in the marine environment. Technical Report Series 247, Vienna.

Kondrachoff, V., Estournel, C., Marsaleix, P., Vehil, R., 1994. Detection of the Rhone River plume using NOAA-AVHRR data. Comparison with hydrodynamic modeling results. Oceanic Remote Sensing and Sea Ice Monitoring 2319, 73–84.

Kowalick, Z., Murty, T.S., 1993. Numerical Modelling of Ocean Dynamics. World Scientific, Singapore.

Krone, R.B., 1962. Flume studies of the transport of sediment in estuarine shoaling processes. Final Report to the San Francisco District US Army Corps of Engineers. University of California, Berkeley.

Laissaoui, A., Abril, J.M., Periáñez, R., García-León, M., García-Montaño, E., 1998. Determining kinetic transfer coefficients for radionuclides in estuarine waters: reference values for ^{133}Ba and effects of salinity and suspended load concentrations. Journal of Radioanalytical Nuclear Chemistry 237, 55–61.

Liu, W.C., Hsu, M.H., Kuo, A.Y., 2002a. Modelling of hydrodynamics and cohesive sediment transport in Tanshui River estuarine system, Taiwan. Marine Pollution Bulletin 44, 1076–1088.

Liu, J.T., Chao, S., Hsu, R.T., 2002b. Numerical modeling study of sediment dispersal by a river plume. Continental Shelf Research 22, 1745–1773.

Lumborg, U., Windelin, A., 2003. Hydrography and cohesive sediment modelling: application to the Romo Dyb tidal area. Journal of Marine Systems 38, 287–303.

Margvelashvily, N., Maderich, V., Zheleznyak, M., 1997. Threetox: a computer code to simulate three dimensional dispersion of radionuclides in stratified water bodies. Radiation Protection Dosimetry 73, 177–180.

Marsaleix, P., Estournel, C., Kondrachoff, V., Vehil, R., 1998. A numerical study of the formation of the Rhone River plume. Journal of Marine Systems 14, 99–115.

Martin, J.M., Thomas, A.J., 1990. Origins, concentrations and distributions of artificial radionuclides discharged by the Rhone River to the Mediterranean Sea. Journal of Environmental Radioactivity 11, 105–139.

Mehta, A.J., Partheniades, E., 1975. An investigation of the depositional properties of flocculated fine sediments. Journal of Hydraulic Research 12, 361–381.

Mitchell, P.I., Vives i Batlle, J., Downes, A.B., Condren, O.M., León-Vintró, L., Sánchez-Cabeza, J.A., 1995. Recent observations on the physico chemical speciation of plutonium in the Irish Sea and the western Mediterranean. Applied Radiation and Isotopes 46, 1175–1190.

Molero, J., Sánchez-Cabeza, J.A., Merino, J., Vives Batlle, J., Mitchell, P.I., Vidal-Cuadras, A., 1995. Particulate distribution of plutonium and americium in surface waters from the Spanish Mediterranean coast. Journal of Environmental Radioactivity 28, 271–283.

Nakano, M., Povinec, P., 2003. Modelling the distribution of plutonium in the Pacific Ocean. Journal of Environmental Radioactivity 69, 85–106.

Nicholson, J., O'Connor, B.A., 1986. Cohesive sediment transport model. Journal of Hydraulic Engineering 112, 621–640.

Nielsen, S.P., 1995. A box model for North-East Atlantic coastal waters compared with radioactive tracers. Journal of Marine Systems 6, 545–560.

Nyffeler, U.P., Li, Y.H., Santschi, P.H., 1984. A kinetic approach to describe trace element distribution between particles and solution in natural aquatic systems. Geochimica Cosmochimica Acta 48, 1513–1522.

Periáñez, R., 2004a. On the sensitivity of a marine dispersion model to parameters describing the transfers of radionuclides between the liquid and solid phases. Journal of Environmental Radioactivity 73, 101–115.

Periáñez, R., 2004b. Testing the behaviour of different kinetic models for uptake/release of radionuclides between water and sediments when implemented in a marine dispersion model. Journal of Environmental Radioactivity 71, 243–259.

Periáñez, R., 1999. Three dimensional modelling of the tidal dispersion of non conservative radionuclides in the marine environment. Application to ^{239,240}Pu dispersion in the eastern Irish Sea. Journal of Marine Systems 22, 37–51.

Periáñez, R., 2000. Modelling the tidal dispersion of ^{137}Cs and ^{239,240}Pu in the English Channel. Journal of Environmental Radioactivity 49, 259–277.

Periáñez, R., 2002. The enhancement of ^{226}Ra in a tidal estuary due to the operation of fertilizer factories and redissolution from sediments: experimental results and a modelling study. Estuarine, Coastal and Shelf Science 54, 809–819.

Periáñez, R., 2003. Kinetic modelling of the dispersion of plutonium in the eastern Irish Sea: two approaches. Journal of Marine Systems 38, 259–275.

Periáñez, R., Martínez-Aguirre, A., 1997. U and Th concentrations in an estuary affected by phosphate fertilizer processing: experimental results and a modelling study. Journal of Environmental Radioactivity 35, 281–304.

Periáñez, R., Abril, J.M., García-León, M., 1996a. Modelling the dispersion of non conservative radionuclides in tidal waters. Part 2: application to ^{226}Ra dispersion in an estuarine system. Journal of Environmental Radioactivity 31, 253–272.

Periáñez, R., Abril, J.M., García-León, M., 1996b. Modelling the dispersion of non conservative radionuclides in tidal waters. Part 1: conceptual and mathematical model. Journal of Environmental Radioactivity 31, 127–141.

Prandle, D., Hargreaves, J.C., McManus, J.P., Campbell, A.R., Duwe, K., Lane, A., Mahnke, P., Shimwell, S., Wolf, J., 2000. Tide, wave and suspended sediment modelling on an open coast, Holderness. Coastal Engineering 41, 237–267.

Radakovitch, O., Charmasson, S., Arnaud, M., Bouisset, P., 1999. ^{210}Pb and caesium accumulation in the Rhone Delta sediments. Estuarine, Coastal and Shelf Science 48, 77–92.

REMOTRANS, 2004. Processes regulating remobilisation, bioavailability, and translocation in marine sediments. EU Project FIS5-1999-00279 Remotrans 000509, Final Report.

Tattersall, G.R., Elliott, A.J., Lynn, N.M., 2003. Suspended sediment concentrations in the Tamar estuary. Estuarine, Coastal and Shelf Science 57, 679–688.

Thill, A., Moustier, S., Garnier, J.M., Estournel, C., Naudin, J.J., Bottero, J.Y., 2001. Evolution of particle size and concentration in the Rhone River mixing zone: influence of salt flocculation. Continental Shelf Research 21, 2127–2140.

Thomas, A.J., 1997. Input of artificial radionuclides to the Gulf of Lions and tracing the Rhone influence in marine surface sediments. Deep Sea Research II 44, 577–595.

Tsimplis, M.N., Proctor, R., Flather, R.A., 1995. A two-dimensional tidal model for the Mediterranean Sea. Journal of Geophysical Research 100, 223–239.

Turner, A., Millward, G.E., 1994. Partitioning of trace metals in a macrotidal estuary. Implications for contaminant transport models. Estuarine, Coastal and Shelf Science 39, 45–58.

Vested, H.J., Baretta, J.W., Ekebjærg, L.C., Labrosse, A., 1996. Coupling of hydrodynamical transport and ecological models for 2D horizontal flow. Journal of Marine Systems 8, 255–267.

Wu, Y., Falconer, R.A., Uncles, R.J., 1998. Modelling of water flows and cohesive sediment fluxes in the Humber Estuary, UK. Marine Pollution Bulletin 37, 182–189.

Xing, J., Davies, A., 1999. The effect of wind direction and mixing upon the spreading of a bouyant plume in a non-tidal regime. Continental Shelf Research 19, 1437–1483.

Zuo, Z., Eisma, D., Gieles, R., Beks, J., 1997. Accumulation rates and sediment deposition in the northwestern Mediterranean. Deep Sea Research II 44, 597–609.